



Coordinative, conformational and motional behaviour of triazine-based ligand strands on binding of Pb(II) cations

Juan Ramírez^a, Adrian-Mihail Stadler^a, Lydia Brelot^b, Jean-Marie Lehn^{a,*}

^a Laboratoire de Chimie Supramoléculaire, Institut de Science et d'Ingénierie Supramoléculaires, Université Louis Pasteur, 8 allée Gaspard Monge, Strasbourg 67083, France

^b Service de rayons X, Institut Le Bel—Université Louis Pasteur, 4, rue Blaise Pascal, 67000 Strasbourg, France

ARTICLE INFO

Article history:

Received 12 March 2008

Received in revised form 15 May 2008

Accepted 30 May 2008

Available online 5 June 2008

Dedicated to Professor James Fraser Stoddart

Keywords:

Self-assembly

Hydrazone ligands

Supramolecular chemistry

Lead

Triazine

ABSTRACT

The coordinative behaviour of two bis(hydrazone)triazine-based ligands in the presence of Pb(II) was investigated. Free ligand, pincer-like and stick-like complexes' X-ray structures are described. The ligands adopt a pyridine-like coordinative behaviour for Pb(II)/ligand molar ratio equal to 1/2 and 1/1, and a pyrimidine-like coordinative behaviour for Pb(II)/ligand molar ratio equal to 2/1. The complexation processes are reversible and may be modulated by external stimuli. They generate conformational and motional behaviour through interconversion of three entities, free ligand, pincer and stick complex.

© 2008 Elsevier Ltd. All rights reserved.

1. Introduction

The structural information contained in a ligand molecule may be implemented in different ways on binding of metal cations, depending on the coordination geometry of the cations, acting as processing algorithm, and on environmental effects (interaction with solvents, counterions).^{1,2} When two or more coordinative behaviours are possible or plausible, and if the manifestation of one of them is exclusive of the others, the former is dominant and the latter(s) is (are) recessive.^{1a,2e} From another point of view, these complexation processes may induce large shape changes in the ligand, thus generating molecular nanomechanical motions, such as contraction/extension of ligand strands.³

We investigated herewith such processes in systems involving the interaction of one kind of metal ion with a triazine-derived hydrazone (hyz) based ligand strand **1**.

The triazine group can be seen as the superimposition⁴ of two six-membered heterocyclic rings: pyrimidine (pym) and pyridine (py) (Fig. 1). A 4,6-disubstituted triazine ring constitutes the central unit of the bis(hydrazone) ligands **1a,b** dealt with here. This structural duality, that keeps both pyrimidine and pyridine structural

features, determines the behaviour of the ligand in the presence of metal ions.

We reported that 1 equiv of such a ligand reacted with 1 equiv of Co(II) and presented dual behaviour modulated by the solvent, leading to a pincer-like complex (in acetonitrile) or to a mixture of pincer-like and grid-like complexes (in nitromethane).⁴ Partial conversions of the grid into pincer (in acetonitrile) and of the pincer into the grid (in nitromethane) were performed. Thus, depending on the nature of the solvent, the ligand adopted either a py-like behaviour in acetonitrile or a mixed py- and pym-like behaviour in nitromethane. We report here the results obtained for the binding of Pb(II) to ligands **1a,b** at various metal/ligand molar ratios, in different solvents.

2. Results and discussion

2.1. Synthesis and structure of the ligands **1**

The two ligands **1a,b** studied here result from the double condensation (Fig. 2) of the corresponding bishydrazines **2a,b** with pyridine-2-carboxaldehyde in ethanol at 30 °C.

The two bis(hydrazino)triazines, **2a** and **2b**, were obtained by reaction of the corresponding dichlorotriazine **3a,b** with methylhydrazine. 2,4-Dichloro-6-phenyl-1,3,5-triazine **3a** was obtained by reaction of 2,4,6-trichloro-[1,3,5]-triazine with phenylmagnesium bromide. 2,4-Dichloro-1,3,5-triazine **3b** was formed by reacting

* Corresponding author.

E-mail address: lehn@isis.u-strasbg.fr (J.-M. Lehn).

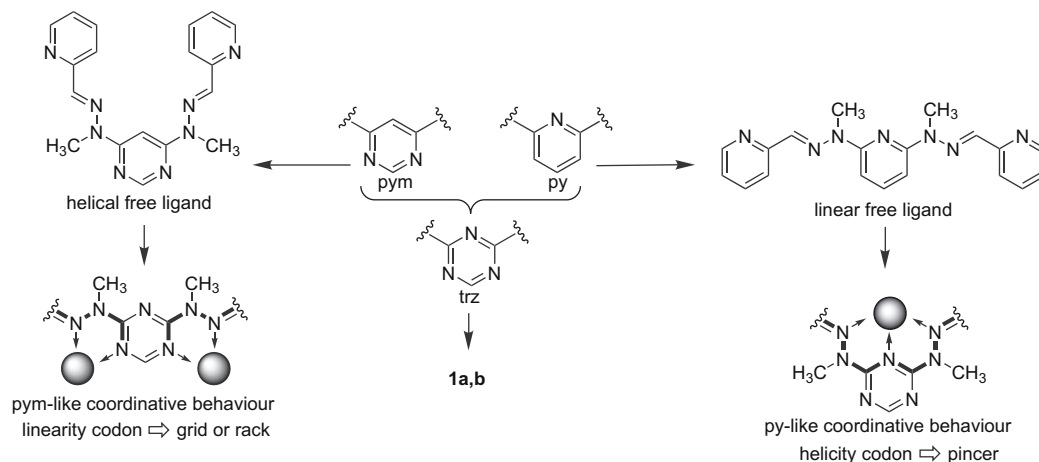


Figure 1. The disubstituted triazine (trz) unit seen as a superposition of pyrimidine (pym) and pyridine (py) units.

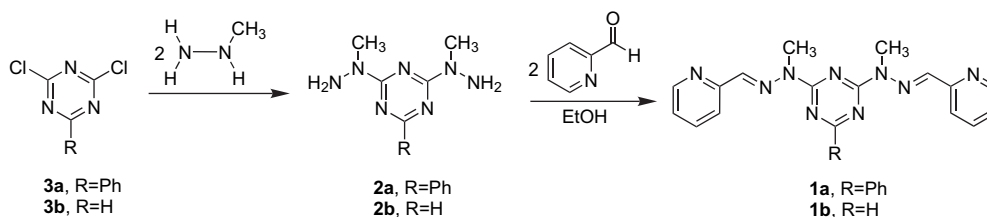


Figure 2. Synthesis of ligands **1a,b** by a double condensation reaction.

N-cyanochloroformamidine (obtained from sodium dicyanamide and hydrochloric acid) with chloromethylene-dimethyl-ammonium (prepared in situ by reaction of POCl₃ with dimethylformamide).

The two ligands **1a,b** were characterized by 1D (¹H and ¹³C) and 2D (¹H–¹H COSY and ¹H–¹H NOESY) NMR spectroscopies. The transoid conformation of the A–B bond in the sequence Nsp²–A–B–Nsp² is known to be strongly favoured over the cisoid one.^{3,5} In **1a,b**, there are two such Nsp²–A–B–Nsp² sequences and there is no ambiguity concerning the transoid conformation of Npy–C2py–Chyz–Nsp²hyz bond. The conformation of the sequence Nsp²hyz–Nsp³hyz–C4trz–N3trz would, in principle, be difficult to establish because there are two Nsp² atoms bound to the same Csp² atom in the triazine ring and two transoid conformations are possible. Ligand **1a** showed in the crystal a ‘linear’ conformation⁶ similar to that adopted by the pyridine based ligands.⁷ In the solid state molecular structure of ligand **1b**, one half of the ligand adopts the ‘linear’ py-mode where the sequence Nsp²hyz–Nsp³hyz–C4trz–N3trz is transoid, the other half of the ligand presenting the pym-mode where Nsp²hyz–Nsp³hyz–C2trz–N1trz is transoid. In both cases, there is a cisoid arrangement of the Nsp²hyz with one of the triazine nitrogen sites. The bond lengths and angles in the two ligands **1a** and **1b** have very similar values and both ligands are almost planar (Fig. 3).

2.2. Structural NMR and X-ray analysis of Pb(II) complexes

Reaction of ligand **1a** with 1 equiv of Pb(II) in acetonitrile results in a complex having a well-defined ¹H NMR spectrum that indicates free rotation of the phenyl ring. Generally, in grid-like complexes of related ligands where the phenyl rotation is impeded,⁸ two kinds of protons G and H are observed by ¹H NMR. This is not the case here. The spectrum obtained is symmetric and the NOE correlations indicate that in solution the conformation of the coordinating ligand corresponds to a pincer-like complex (Fig. 4).

The NOE correlations (D,E) and (E,F) confirm the passing from the transoid conformation of the C4trz–Nsp³hyz, C2trz–Nsp³hyz and Chyz–C2py bonds in the free ligand to their cisoid conformation as a consequence of coordination by Pb(II). Thus, for a metal/ligand molar ratio 1/1, Pb(II) generates, in acetonitrile, a pincer-like complex, as was also the case for Co(II).

The X-ray structure of the Pb(II) pincer-like complex of ligand **1a**, crystallized from acetonitrile, has been determined and it confirmed the pincer-like structure proposed on the basis of the 2D NMR. The crystal contains two crystallographically distinct types of dimers of pincers, but the conformations of the ligand are almost identical in both of them. The two pincers of a dimer are identical.

In the first type of pincer two triflate anions are coordinated to the Pb(II) cation in an axial mode at less than 2.7 Å (Fig. 5). The distance between the Pb(II) and a third O atom (O5, not shown in Fig. 5) that belongs to a triflate of the second pincer (not shown in Fig. 5) of the dimer (not shown in Fig. 5) is about 2.93 Å. Pb–N and

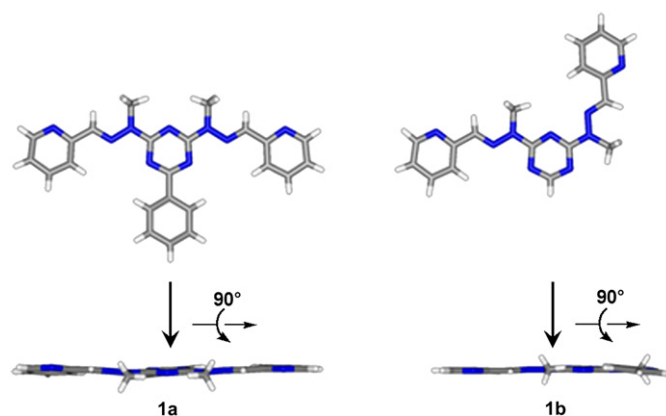


Figure 3. X-ray crystallographic solid state molecular structures of ligands **1a** and **1b**.

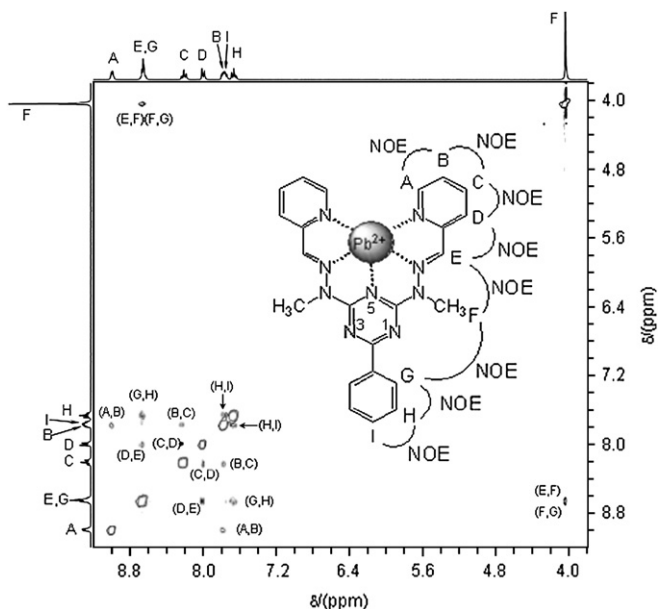


Figure 4. ^1H - ^1H NOESY spectrum (300 MHz, 25 °C) of the complex **Pb1a**(OTf) $_2$ in CD_3CN .

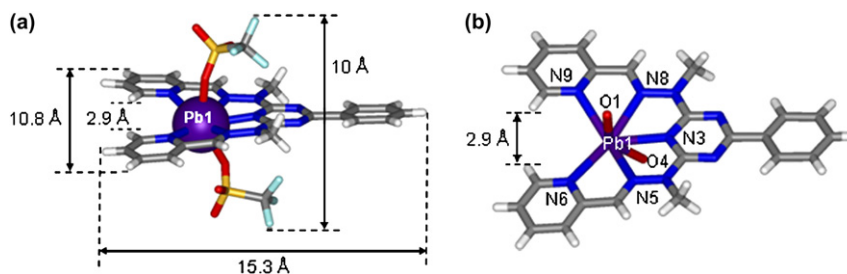


Figure 5. Solid state molecular structure of the first type of Pb(II) pincer complex of ligand **1a** crystallized from acetonitrile; only one pincer of the dimer is shown: (a) side view; (b) top view and numbering of the atoms.

Table 1
Lengths of the coordination bonds in the Pb(II) pincer complexes of ligand **1a**

Crystallized from CH_3CN				Crystallized from CH_3NO_2	
First type (Fig. 5)		Second type (Fig. 6)		(Fig. 7)	
Bond	Length (Å)	Bond	Length (Å)	Bond	Length (Å)
N_{py} Pb1–N6	2.73	Pb2–N15	2.69	Pb1–N6	2.71
N_{py} Pb1–N9	2.70	Pb2–N18	2.73	Pb1–N9	2.74
N_{hyz} Pb1–N8	2.66	Pb2–N14	2.63	Pb1–N5	2.61
N_{hyz} Pb1–N5	2.67	Pb2–N17	2.67	Pb1–N8	2.67
N_{trz} Pb1–N3	2.57	Pb2–N12	2.54	Pb1–N3	2.54
Pb1–O4	2.70	Pb2–O7	2.84	Pb–O1	2.40
Pb1–O1	2.56	Pb2–O8	2.84	Pb1–O2	2.81
Pb1–O5	2.93	Pb2–O13	2.45		

Pb–O distances are listed in Table 1. The Pb–Pb distance in this dimer is 6.55 Å.

The second type of Pb(II) pincer-like complex of ligand **1a**, crystallized from acetonitrile (Fig. 6), is very similar to the first type of pincer. The ligand is almost planar and coordinates in a penta-dentate mode. Two pincers are bound by two triflate anions that act as bridging ligands thanks to oxygen atoms, to form a dimer. Each of the two pincers presents an additional water molecule bound to Pb(II), thus the coordination number of Pb(II) is equal to 8. The lengths of the coordination bonds are given in Table 1.

In the case of Co(II), the self-assembly of the complex is modulated by the nature of the solvent: the lesser coordinating one (nitromethane) increases the fraction of grid, while the more coordinating solvent (acetonitrile) gave the pincer.⁴ With this in mind, we crystallized the complex of **1a** with Pb(II) from nitromethane. Determination of the solid state molecular structure revealed a pincer-like complex similar to those above described. In the case of the Co(II) pincer, the smaller metal ion induced a helical pitch of the ligand,⁴ while here, as Pb(II) is appreciably larger, the ligand is almost planar. The axial positions are occupied by a water molecule and by the oxygen of a triflate. The difference between the Pb–O_{water} and Pb–O_{triflate} bonds is about 0.4 Å (Table 1 and Fig. 7). The coordination number of Pb(II) is 7 and the cation is slightly out of the ligand plane.

In all three pincer-type complexes of ligand **1a**, the average Pb–N distances increase in the sequence: Pb–N_{trz} (2.55 Å) < Pb–N_{hyz} (2.65 Å) < Pb–N_{py} (2.72 Å). The Pb–O distances lie between 2.39 Å and 2.93 Å.

For ligand **1b**, the replacement of the phenyl ring of **1a** by a hydrogen should not change the coordinative capacities. Indeed, the molecular structure in the solid state of the complex obtained from 1 equiv of **1b** and 1 equiv of Pb(II) in acetonitrile, is a dimer of pincers, similar to that formed by **1a** in similar conditions and can be described as $[\text{Pb}_2(\text{1b})_2(\mu\text{CF}_3\text{SO}_3)_2(\text{H}_2\text{O})_2]^{2+}$ (Table 2 and Fig. 8). The two pincer-like complexes contained in the dimer are slightly different and are connected by two bridging triflate anions.

The coordination distances in the Pb(II) complexes of ligands **1a** and **1b** are similar. For the Pb(II) pincer-like complex of ligand **1b**,

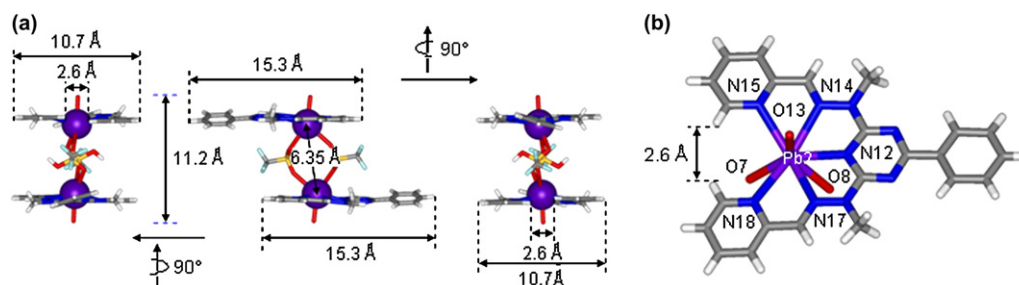


Figure 6. Solid state molecular structure of the second type of Pb(II) pincer complex of ligand **1a** crystallized from acetonitrile: (a) side views; (b) top view and numbering of the atoms.

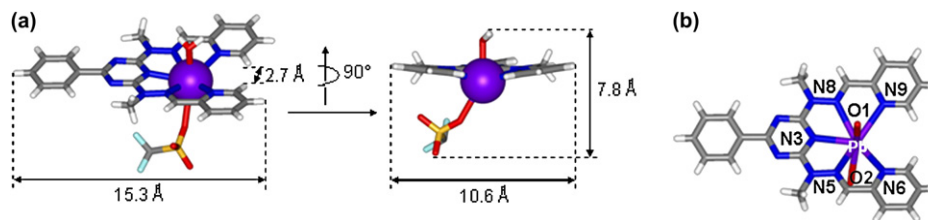


Figure 7. Pincer of ligand **1a** crystallized from nitromethane: (a) side views; (b) numbering of the atoms.

the average Pb–N distances increase in the following order Pb–N_{trz} (2.62 Å) < Pb–N_{hyz} (2.69 Å) < Pb–N_{py} (2.74 Å), while for the stick-like complex of the same ligand the order is Pb–N_{py} (2.54 Å) < Pb–N_{hyz} (2.60 Å) ≈ Pb–N_{trz} (2.61 Å).

Treatment of ligand **1b** with 2 equiv of Pb(II) or of the pincer of this same ligand with 1 equiv of Pb(II) gives a dinuclear linear stick-like complex,⁹ X-ray crystal structure of which has been determined. One Pb(II) cation is partially out of the plane. Each of the two Pb(II) cations is coordinated by three sp² N atoms (N_{py}, N_{hyz},

N_{trz}) and by three oxygen atoms from triflate anions. The ligand length is about 18.1 Å and the Pb–Pb distance is about 6.9 Å. In the solid state, the dinuclear sticks are connected by triflate anions and generate a polymeric architecture (Table 2 and Fig. 9).

2.3. Multiple coordination behaviour

Two types of coordinative behaviour of ligands **1a,b** may be considered here: solvent-dependent and stoichiometry-dependent.

Table 2

Length of the coordination bonds in the dimeric Pb(II) pincer complex of ligand **1b**, crystallized from acetonitrile, and in the corresponding stick-like complex

	Pb(II) pincer of 1b				Pb(II) stick of 1b			
	Pb1		Pb2		Pb1		Pb2	
	Bond	Length (Å)	Bond	Length (Å)	Bond	Length (Å)	Bond	Length (Å)
N _{py}	Pb1–N9	2.79	Pb2–N15	2.73	Pb1–N6	2.55	Pb2–N9	2.54
N _{py}	Pb1–N6	2.71	Pb2–N18	2.74				
N _{hyz}	Pb1–N5	2.69	Pb2–N14	2.67	Pb1–N5	2.65	Pb2–N8	2.55
N _{hyz}	Pb1–N8	2.69	Pb2–N17	2.70				
N _{trz}	Pb1–N3	2.61	Pb2–N12	2.63	Pb1–N2	2.62	Pb2–N3	2.61
	Pb1–O1	2.44	Pb2–O2	2.46	Pb1–O1	2.58	Pb2–O8	2.81
	Pb1–O3	2.81	Pb2–O4	2.89	Pb1–O7	2.51	Pb2–O12	2.67
	Pb1–O6	2.96	Pb2–O7	2.80	Pb1–O4	2.70	Pb2–O10	2.51

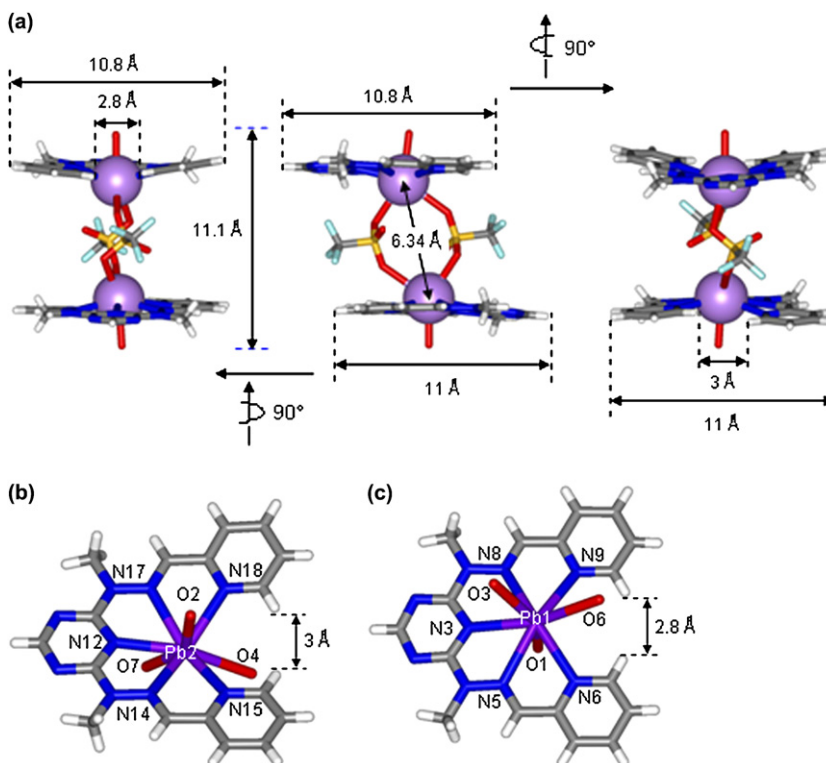


Figure 8. Solid state molecular structure of the Pb(II) pincer dimer complex $[\text{Pb}_2(\mathbf{1b})_2(\mu\text{CF}_3\text{SO}_3)_2(\text{H}_2\text{O})_2]^{2+}$: (a) side view of the dimer; (b) and (c) top views and numbering of atoms in each of the two pincers of the dimer.

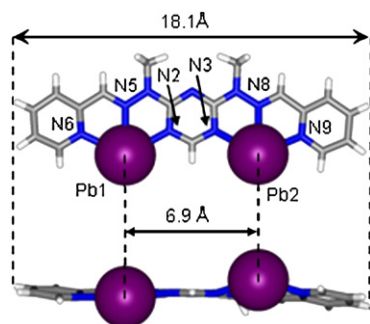


Figure 9. Solid state molecular structure of the dinuclear Pb(II) stick complex of ligand **1b** (triflate anions were omitted for clarity).

For a Pb(II)/**1** molar ratio of 1/1, the nature of the solvent has no influence on the coordinative behaviour of ligand **1b**, as both in acetonitrile and nitromethane the pincer-like complex is formed. On the other hand, with Co(II), nitromethane induces the formation of

both pincer- and grid-like complex while acetonitrile stabilizes the pincer-like complex. The coordination plasticity required for undergoing structural adaptation in response to solvent nature, although contained in the ligand, is thus not observed for Pb(II) for an equimolar metal/ligand ratio. Only the py-mode is observed, while for Co(II) the solvent-dependent dual mode is expressed (Fig. 10).

This dual complexation behaviour results from the fact that the triazine unit in the ligands **1a,b** may operate either in a py-like or in a pym-like coordination mode, one of them being dominant and the other recessive, depending on conditions (nature of the metal ion, solvent, and stoichiometry).

The structural plasticity of ligands **1** translates into their diverse coordinative behaviour depending on the nature of cation, of the solvent but also, for the same cation and solvent, on the M(II)/L stoichiometry variations. With this latter aspect in mind, we investigated the behaviour of ligands **1a,b** in presence of an increasing amount of Pb(II).

Titration of ligand **1a** by Pb(II) triflate has been followed by ^1H NMR (Fig. 11). For a molar ratio Pb(II)/**1a** 1/2, a well-defined

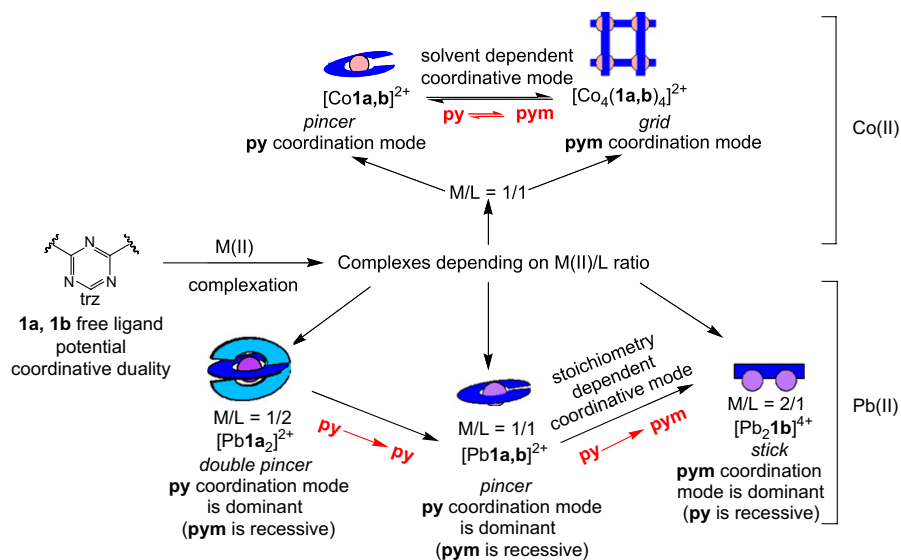


Figure 10. Coordinative modes of the triazine ligands **1a** and **1b** as determined by the nature of the cation, solvent and stoichiometry.

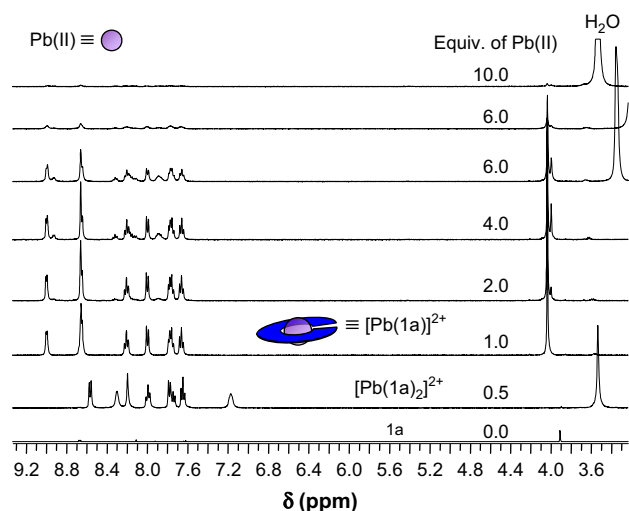


Figure 11. Titration of ligand **1a** by Pb(II) triflate in CD_3CN , followed by 400 MHz ^1H NMR. Due to the low solubility of the free ligand **1a** in CD_3CN , the intensity of its signals in the bottom spectrum is weak.

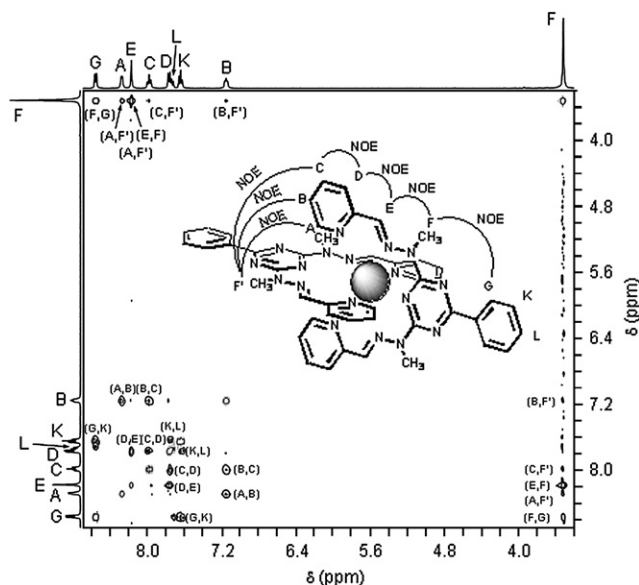


Figure 12. ^1H - ^1H NOESY spectrum of complex $[\text{Pb}(\mathbf{1a})_2]^{2+}$ in CD_3CN .

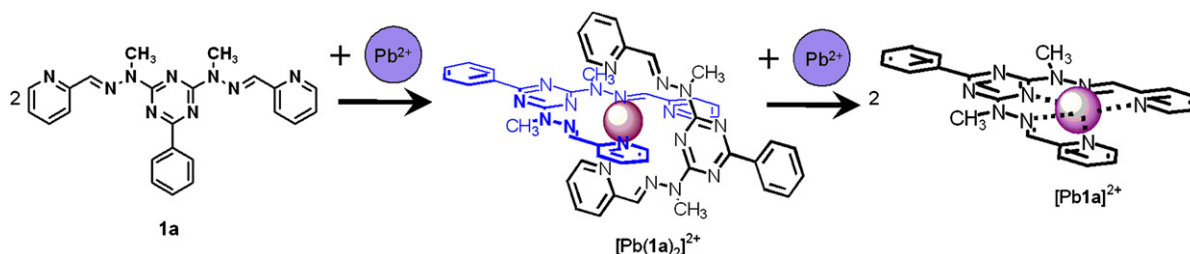


Figure 13. Successive formation of double-pincer and pincer-like Pb(II) complexes by ligand **1a** at Pb(II)/**1a** molar ratios 1/2 and 1/1.

spectrum has been recorded and it should correspond to the complex cation $[\text{Pb}(\mathbf{1a})_2]^{2+}$. Such double pincers were previously described for a quinquepyridine ligand.¹⁰ At a molar ratio of 1/1, the pincer-like complex $[\text{Pb}\mathbf{1a}]^{2+}$ above characterized has been observed. Further addition of Pb(II) slowly produced changes in the NMR spectrum, thus showing a certain kinetic stability of the pincer-like complex. The excess Pb(II) finally transforms the pincer most likely into the stick-like complex $[\text{Pb}_2\mathbf{1a}]^{4+}$, that precipitates and cannot be observed by ^1H NMR. However, the formation of its analogue complex $[\text{Pb}_2\mathbf{1b}]^{4+}$ (see above) supports the assignment of the stick structure to this complex, which is less soluble due to the phenyl ring.

For the complex observed at 0.5 equiv of Pb(II), the NOESY spectrum (Fig. 12), confirms that **1a** acts as pentadentate ligand. The NOE correlation between the protons of methyl group F and the proton G in the *ortho* position of the phenyl ring, between the methyl group F' and the protons A, B and C of pyridine strongly suggest the positioning of the ligands as in a double-pincer complex. The conversion of ligand **1a** first into the double-pincer and subsequently into the pincer-like complex are represented in Figure 13. Considering the ability of ligand **1a** to adopt either a py- or a pym-like coordination mode, at Pb(II)/**1a** molar ratio of 1/2 and 1/1, it acts solely in py-mode and the preference for the py-mode is conserved at Pb(II)/**1a** 1/1, independently of the solvent. The pym-like behaviour is recessive. In comparison, with Co(II), both the py- and pym-like modes are observed simultaneously.⁴ Thus, from 2/1 to 1/1 stoichiometry there are two successive py-like steps (Fig. 10). From 1/1 to 1/2, the mode changes from py-like (pincer⁷) to pym-like (stick⁹), so the dual behaviour is not simultaneous, but successive (Fig. 13).

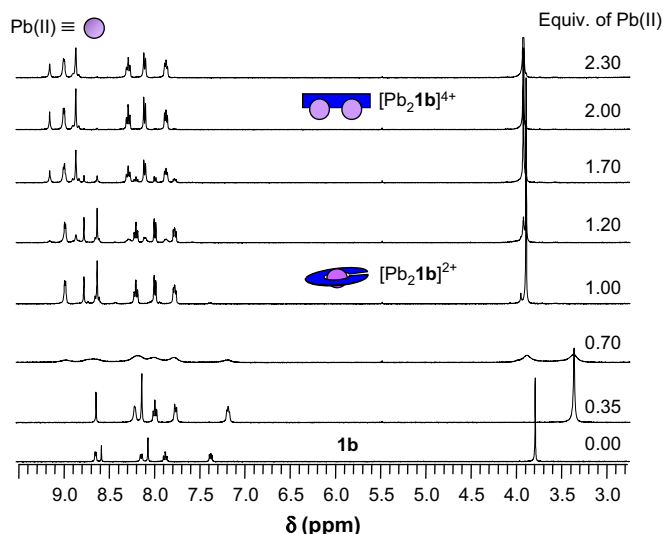


Figure 14. ^1H NMR observation of the titration of ligand **1b** by Pb(II) triflate in CD_3CN .

Also the couple Pb(II)/**1b** displays a stoichiometry-dependent behaviour. NMR titration of ligand **1b** by Pb(II) triflate in CD_3CN is shown in Figure 14. At Pb(II)/**1b** molar ratio of 1/1 and 2/1, the pincer-like and stick-like complexes, respectively, formed. Thus, from 1/1 to 2/1, the coordinative behaviour changes from a py-like to a pym-like mode, in a successive dual sequence. At 0.35 equiv Pb(II) (\approx Pb(II)/**1b** 1/3), a well-defined spectrum is obtained. Although crystallization attempts were unsuccessful, on the basis of the NMR titration and of the NOESY spectrum indicating the coordinated, pincer-like conformation of **1b**, we can assume that this complex corresponds to $[\text{Pb}(\mathbf{1b})_3]^{2+}$.

2.4. Motional dynamic behaviour

The conversion of compounds **1a** and **1b** from their shape in the pincer-like complexes to their shape in the stick-like complexes Pb(II) represents a metal ion induced modulation of nano-mechanical motions of extension/contraction type.³ Reversible motion may be generated by successive complexation/decomplexation steps via implementation of a competing ligand and external stimuli. The binding of Pb(II) by the ligands **1a,b** is sufficiently labile to allow complexing of Pb(II) by a stronger ligand such as tris(2-aminomethyl)amine, tren.¹¹ Indeed, by adding 1 equiv of tren to the complex $[\text{Pb}_2\mathbf{1b}]^{4+}$, the shape of the ligand was converted from the extended form in the stick-like complex $[\text{Pb}_2\mathbf{1b}]^{4+}$ to the curved form in the pincer-like complex $[\text{Pb}\mathbf{1b}]^{2+}$ (Fig. 15). In terms of amplitude, depending on the reference protons considered, this conversion represents a variation from 10.6 Å (for the proton on C6py) to 9 Å (for the proton on C5py) or 7.2 Å (for the proton on C4py) (Fig. 16). These processes represent a reversible interconversion between the two complexes and induce the

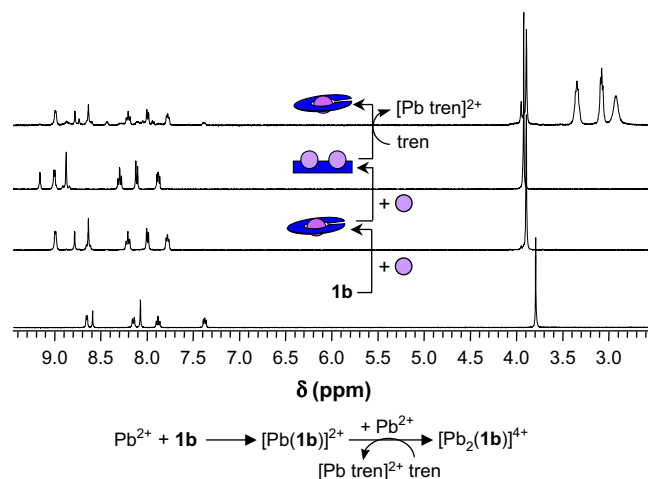


Figure 15. Interconversion of Pb(II) complexes of ligand **1b** modulated by the ligand tren $\text{N}(\text{CH}_2\text{CH}_2\text{NH}_2)_3$ in CD_3CN .

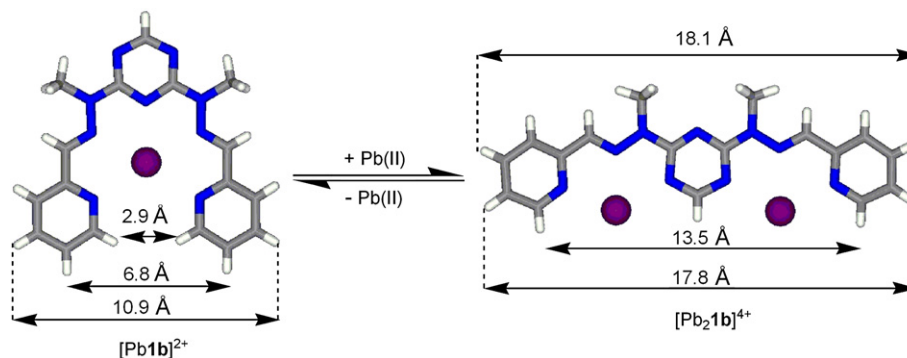


Figure 16. Quantitative expression of distances in extension/contraction molecular motions of pincer and stick Pb(II) complexes of the ligand **1b**.

motional changes corresponding to the changes in shape of ligand in the two states.

Subsequent protonation of tren will produce the release of Pb(II) cations that will coordinate again with the ligand thus generating the complex existing prior to tren addition. Indeed, after the formation of the pincer-like $[\text{Pb1a}]^{2+}$ complex, addition of 0.5 equiv of tren led to encapsulation of Pb(II) ions, thus producing the double-pincer complex $[\text{Pb1b}_2]^{2+}$. Thereafter, addition of 1.5 equiv of $\text{CF}_3\text{SO}_3\text{H}$ to the solution resulted in the regeneration of the pincer-like complex (Fig. 17). These processes represent a protonation-induced, tren-mediated reversible interconversion of the two coordination architectures.

3. Conclusions

The two triazine-based ligands **1a,b** present a dual complexation behaviour towards Pb(II) cation, consisting in their ability to

act in a py-like mode or in a pym-like mode depending on the Pb(II)/ligand molar ratio. Moreover, the process may be controlled by external stimuli. As a result, the ligands undergo changes in shape, representing nanomechanical molecular motions of extension/contraction type that may be reversibly modulated via external stimuli. Finally, the dependence of ligand behaviour on the nature of the cation gives access to diverse multiple coordinative modes as well as to specific motional changes.

4. Experimental section

4.1. General

2,4-Dichloro-6-phenyl-1,3,5-triazine,¹² 2,4-dichloro-1,3,5-triazine¹³ and $\text{Pb}(\text{OTf})_2$ ¹⁴ were prepared as previously described. The following reagents were purchased from commercial sources: CH_3NO_2 (Aldrich), CD_3CN , CDCl_3 (Eurisotop).

Solution ^1H (400 MHz) and ^{13}C (100 MHz) NMR spectra were recorded with a Bruker Ultrashield Avance 400 instrument and ^1H (300 MHz) NMR, COSY, NOESY spectra were recorded on a Bruker AM 300 spectrometer. The solvent signal was used as an internal reference for ^1H NMR (CD_2HCN , $\delta=1.94$ ppm; CHCl_3 , $\delta=7.24$ ppm) and ^{13}C NMR (CHCl_3 , $\delta=77.2$ ppm) spectra. The following notation is used for the ^1H NMR spectral splitting patterns: singlet (s), doublet (d), triplet (t), multiplet (m). 2D NMR used experiments were: COSY (Correlation Spectroscopy) and NOESY (Nuclear Overhauser Enhancement Spectroscopy).

For crystal structure determinations, the crystals were obtained by diffusion–recrystallization by using the appropriate solvent and non-solvent. The crystals were placed in oil, a single crystal was selected, mounted on a glass fibre and placed in a low-temperature N_2 stream.

4.1.1. Ligands

4.1.1.1. 2,4-Bis[*N*-methyl-*N'*-(pyridin-2-yl)methylidene]hydrazino]-6-phenyltriazine **1a**. A stirred solution of **2a** (40.8 mg, 0.16 mmol) and pyridine-2-carboxaldehyde (32 μL , 0.32 mmol) in ethanol (5 mL) was heated at 30 °C for 15 h. The white solid that precipitated was isolated by filtration, washed with ethanol and dried under vacuum. Yield: 50.8 mg (72%). Mp 231 °C. ^1H NMR (CDCl_3 , 400 MHz): $\delta=8.62$ (d, $J=4.4$ Hz, 2H), 8.58 (d, $J=7$ Hz, 2H), 8.33 (d, $J=7.7$ Hz, 2H), 8.08 (s, 2H), 7.79 (td, $J=7.3$, 1.5 Hz, 2H), 7.59–7.49 (m, 3H), 7.29 (ddd, $J=7.3$, 4.8, 1.1 Hz, 2H), 3.88 (s, 6H) ppm. ^{13}C NMR (CDCl_3 , 100 MHz): $\delta=154.7$, 149.4, 140.8, 136.5, 136.5, 132.4, 129.0, 128.6, 123.8, 120.6, 31.2 ppm. ES-MS (m/z): 424.2002 (calcd for $[\text{1aH}]^+=[\text{C}_{23}\text{H}_{22}\text{N}_9]^+$: 424.1993), 430.2092 (calcd for $[\text{1aLi}]^+=[\text{C}_{23}\text{H}_{21}\text{N}_9\text{Li}]^+$: 430.2075), 446.1836 (calcd for $[\text{1aNa}]^+=[\text{C}_{23}\text{H}_{21}\text{N}_9\text{Na}]^+$: 446.1812).

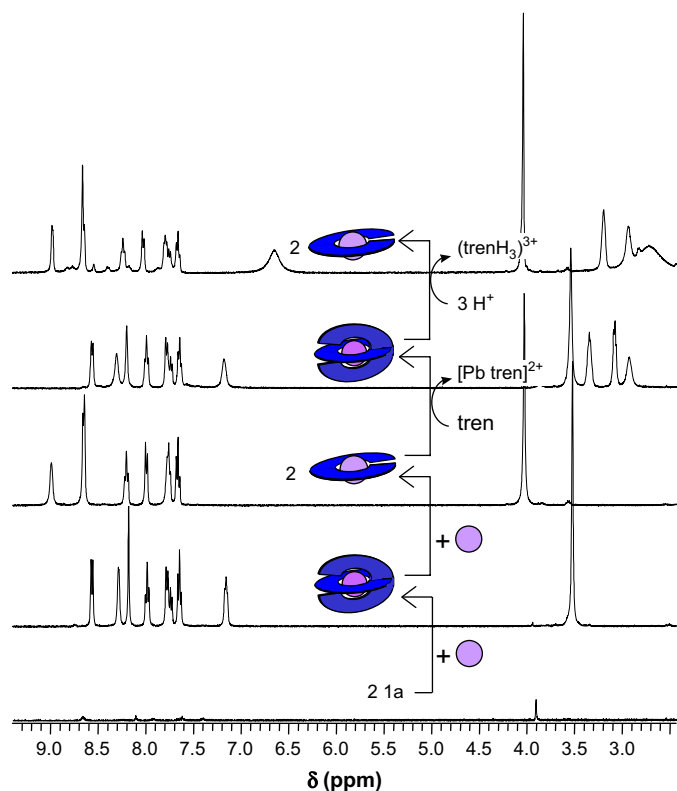


Figure 17. Proton-modulated reversible interconversion of pincer-like and double-pincer complexes of ligand **1a** mediated by the competing ligand tren, in CD_3CN . Due to the low solubility of the free ligand **1a** in CD_3CN , the intensity of its signals in the bottom spectrum is weak.

4.1.2. 2,4-Bis[*N*-methyl-*N'*-(pyridin-2-yl)methylidene]hydrazino]-triazine **1b**

A stirred solution of 2,4-bis(*N*-methylhydrazino)-1,3,5-triazine **2b** (340 mg, 2.0 mmol, 1 equiv) and pyridine-2-carboxaldehyde (0.38 mL, 4.0 mmol, 2 equiv) in ethanol (30 mL) was stirred at room temperature for 12 h. The white solid that precipitated was isolated by filtration, washed with ethanol and Et₂O and dried under vacuum. Yield: 623 mg (89%). Mp 230–231 °C. ¹H NMR (CDCl₃, 400 MHz): δ=8.64 (s, 1H), 8.58 (ddd, *J*=5.0, 1.6, 0.8 Hz, 2H), 8.20 (d, *J*=7.5 Hz, 2H), 8.02 (s, 2H), 7.73 (ddd, *J*=7.5, 3.7, 0.8 Hz, 2H), 7.25 (dd, *J*=7.3, 1.6 Hz, 2H), 3.75 (s, 6H) ppm. ¹³C NMR (CDCl₃, 100 MHz): δ=164.9, 154.2, 149.5, 148.6, 141.7, 136.7, 123.9, 120.8, 30.9 ppm. ES-MS (*m/z*): 348.1642 (calcd for [**1bH**]⁺=[C₁₇H₁₈N₉]⁺: 348.1680), 354.1726 (calcd for [**1bLi**]⁺=[C₁₇H₁₇N₉Li]⁺: 354.1762), 370.1462 (calcd for [**1bNa**]⁺=[C₁₇H₁₇N₉Na]⁺: 370.1499). Single crystals were obtained by liquid/liquid diffusion of CH₃CN in a CHCl₃ solution of **1b**. The solid state structure was determined by X-ray diffraction. Crystallographic data: formula: C₁₇H₁₇N₉=**1b**; *M*=347.40 g mol^{−1}; crystal system: triclinic; space group: $\bar{P}1$ (no. 2); *a*=8.008(2), *b*=10.508(3), *c*=10.804(3) Å; α=96.042(9)°, β=109.880(3)°, γ=95.836(4)°; *V*=841.0(4) Å³; *Z*=2; ρ_{calcd}=1.372 g cm^{−3}; μ=0.006 mm^{−1}; *F*(000)=364; *T*=395 K; radiation λ=0.26470 Å; 3.8°≤θ≤11.7°; *hkl* limits: −11, 11/−16, 16/−16, 16; total data: 11007; unique data: 4915; *R*(int): 0.024; observed data with *I*>2σ(*I*): 4379; *N*_{ref}=4915; *N*_{par}=303; *R*=0.0473; *wR*2=0.1335; *GOF*=1.09; min. and max. residual density: −0.25/0.42 e Å^{−3}.

4.1.3. 2,4-Bis(*N*-methylhydrazino)-2-phenyl-1,3,5-triazine **2a**

A stirred solution of 2,4-dichloro-6-phenyl-1,3,5-triazine (1.05 g, 4.2 mmol) and methylhydrazine (0.98 mL, 18.3 mmol) in ethanol (20 mL) was heated to reflux for 2 h. The white solid that precipitated on cooling was isolated by filtration, washed with ethanol and dried under vacuum. Yield: 0.45 g (39%). Mp 155 °C. ¹H NMR (CDCl₃, 400 MHz): δ=8.39 (dd, *J*=8.2 Hz, *J*=1.6 Hz, 2H), 7.50–7.40 (m, 3H), 4.57 (s, 4H), 3.40 (s, 6H) ppm. ¹³C NMR (CDCl₃, 100 MHz): δ=170.2, 166.4, 137.3, 131.5, 128.5, 128.3, 37.7 ppm.

4.1.4. 2,4-Bis(*N*-methylhydrazino)-1,3,5-triazine **2b**

To a stirred solution of 2,4-dichloro-1,3,5-triazine (478.5 mg, 2.8 mmol) in dichloromethane (20 mL) cooled at −10 °C was added methylhydrazine (0.67 mL, 12.5 mmol). The cooling was removed and the mixture was stirred at room temperature for 19 h. The solid that precipitated was removed by filtration and the resulting solution was concentrated under vacuum to give 0.50 g of white solid (93%). Mp 107–108.5 °C. ¹H NMR (CDCl₃, 400 MHz): δ=8.15 (s, 1H), 4.27 (s, 4H), 3.30 (s, 6H) ppm. ¹³C NMR (CDCl₃, 100 MHz): δ=165.1, 165.0, 37.8 ppm.

4.1.5. Complexes

4.1.5.1. Pb(II) pincer-like complex of ligand **1a** from acetonitrile. A

solution of ligand **1a** (22.1 mg, 0.052 mmol) and Pb(CF₃SO₃)₂ (26.4 mg, 0.052 mmol) in CH₃CN (4 mL) was stirred at 45 °C for 1 h. ¹H NMR (CD₃CN, 400 MHz): δ=8.95 (d, *J*=4.15 Hz, 2H), 8.64–8.60 (m, 4H), 8.16 (td, *J*=1.6 Hz, *J*=7.8 Hz, 2H), 7.96 (d, *J*=7.8 Hz, 2H), 7.75–7.70 (m, 3H), 7.62 (t, *J*=7.6 Hz, 2H), 3.99 (s, 6H) ppm. 2D NMR: COSY, NOESY. Single crystals were obtained by vapor/liquid diffusion of diisopropylether into a CH₃CN solution. The solid state structure was determined by X-ray diffraction. Crystallographic data: formula: C₁₀₀F₂₄N₃₆O₂₆Pb₄S₈=4Pb**1a**(CF₃SO₃)₂·2H₂O; *M*=3662.72 g mol^{−1}; crystal system: triclinic; space group: $\bar{P}1$ (no. 2) *a*=13.3650(5), *b*=17.8270(8), *c*=19.6030(8) Å; α=108.878(4)°, β=102.327(3)°, γ=103.518(2)°; *V*=4079.2(3) Å³; *Z*=1; ρ_{calcd}=1.525 g cm^{−3}; μ=4.311 mm^{−1}; *F*(000)=1816; *T*=173 K;

radiation λ=0.26470 Å; 2.69°≤θ≤27.52; *hkl* limits: −17, 10/−20, 23/−19, 20; total data: 18,758; unique data: 15,061; *R*(int): 0.060; observed data with *I*>2σ(*I*): 7817; *N*_{ref}=15,061; *N*_{par}=838; *R*=0.0736; *wR*2=0.2151; *GOF*=1.008; min. and max. residual density: −2.573/2.179 e Å^{−3}.

4.1.6. Pb(II) pincer-like complex of ligand **1a** from nitromethane

A solution of ligand **1a** (60.60 mg, 0.143 mmol) and Pb(CF₃SO₃)₂ (72.31 mg, 0.143 mmol) in CH₃NO₂ (27 mL) was heated until complete dissolution. Single crystals were obtained on slow cooling. The solid state structure was determined by X-ray diffraction. Crystallographic data: formula: C₂₆H₂₆F₆N₁₀O₉PbS₂=Pb**1a**(CF₃SO₃)₂·CH₃NO₂·H₂O; *M*=1007.88 g mol^{−1}; crystal system: monoclinic; space group: *P*2₁/*c* (no. 14); *a*=10.8541(2), *b*=22.1370(3), *c*=16.9205(3) Å; β=118.079(1)°; *V*=3587.09(1) Å³; *Z*=4; ρ_{calcd}=1.866 g cm^{−3}; μ=4.915 mm^{−1}; *F*(000)=1968; *T*=173 K; radiation: Mo Kα (λ=0.71073 Å); 1.6°≤θ≤30.0°; *hkl* limits: −15, 14/−31, 28/−23, 23; total data: 28,744; unique data: 10,321; *R*(int): 0.072; observed data with *I*>2σ(*I*): 7437; *N*_{ref}=10,321; *N*_{par}=462; *R*=0.0530; *wR*2=0.1485; *GOF*=1.02; min. and max. residual density: −4.43/2.72 e Å^{−3}.

4.1.7. Pb(II) pincer-like complex of ligand **1b**

A solution of ligand **1b** (46.49 mg, 0.13 mmol) and Pb(CF₃SO₃)₂ (67.63 mg, 0.13 mmol) in CH₃NO₂ (18 mL) was stirred for 10 min at room temperature. ¹H NMR (CD₃CN, 400 MHz): δ=8.94 (d, *J*=4.1 Hz, 2H), 8.74 (s, 1H), 8.59 (s, 2H), 8.17 (t, *J*=7.8 Hz, 2H), 7.95 (d, *J*=7.3 Hz, 2H), 7.74 (t, *J*=6.2, 2H), 3.85 (s, 6H) ppm. NMR 2D: COSY and NOESY. Single crystals were obtained by vapor/liquid diffusion of diisopropylether into a CH₃NO₂ solution. The solid state structure was determined by X-ray diffraction. Crystallographic data: formula: C₃₈H₃₄F₁₂N₁₈O₁₄Pb₂S₄=2Pb**1b**(CF₃SO₃)₂·2H₂O; *M*=1737.45; crystal system: triclinic; space group: $\bar{P}1$ (no. 2); *a*=9.0800(2), *b*=13.6285(4), *c*=23.3552(6) Å; α=85.630(1), β=87.795(2), γ=78.804(2) Å; *V*=2826.06(13) Å³; *Z*=2; ρ_{calcd}=2.042 g cm^{−3}; μ=6.214 mm^{−1}; *F*(000)=1672; *T*=173 K; radiation: Mo Kα (λ=0.71073 Å); 1.5°≤θ≤29.1°; *hkl* limits: −12, 12/−14, 18/−28, 31; total data: 37,832; unique data: 15,027; *R*(int): 0.068; observed data with *I*>2σ(*I*): 9834; *N*_{ref}=15,027; *N*_{par}=797; *R*=0.0433; *wR*2=0.0961; *GOF*=0.97; min. and max. residual density: −2.31/1.85 e Å^{−3}.

4.1.8. Pb(II) stick-like complex of ligand **1b**

Ligand **1b** (3.28 mg, 9.4 μmol) and Pb(CF₃SO₃)₂ (10 mg, 19.8 μmol) were stirred in CD₃CN (0.65 mL) until complete dissolution. ¹H NMR (CD₃CN, 300 MHz): δ=9.12 (s, 1H), 8.96 (d, *J*=4.1 Hz, 2H), 8.83 (s, 2H), 8.25 (t, *J*=7.5 Hz, 2H), 8.07 (d, *J*=7.5 Hz, 2H), 7.83 (t, *J*=7.0 Hz, 2H), 3.88 (s, 6H) ppm. Single crystals were obtained by vapor/liquid diffusion of diisopropylether into this solution. The solid state structure was determined by X-ray diffraction. Crystallographic data: formula: C₂₁H₁₇F₁₂N₉O₁₂Pb₂S₄=Pb₂**1b**(CF₃SO₃)₄; *M*=1358.12; crystal system: monoclinic; space group: *P*2₁/*c* (no. 13); *a*=19.8659(6), *b*=13.6821(4), *c*=16.3068(4) Å; β=113.921(2)°; *V*=4051.6(2) Å³; *Z*=4; ρ_{calcd}=2.227 g cm^{−3}; μ=8.625 mm^{−1}; *F*(000)=2552; *T*=173 K; radiation: Mo Kα (λ=0.71073 Å); 1.5°≤θ≤27.5°; *hkl* limits: −25, 19/−17, 16/−14, 21; total data: 24,074; unique data: 8923; *R*(int): 0.062; observed data with *I*>2σ(*I*): 7181; *N*_{ref}=8923; *N*_{par}=502; *R*=0.0846; *wR*2=0.2236; *GOF*=1.18; min. and max. residual density: −2.69/3.62 e Å^{−3}.

CCDC-680765 (**1b**), CCDC-680764 (stick-like complex Pb₂**1b**(OTf)₄), CCDC-680767 (pincer-like complex Pb**1b**(OTf)₂), CCDC-681285 (pincer-like complex Pb**1a**(OTf)₂ crystallized from CH₃CN) and CCDC-680766 (pincer-like complex Pb**1a**(OTf)₂ crystallized from CH₃NO₂) contain the supplementary crystallographic data for this paper. These data can be obtained free of charge from

the Cambridge Crystallographic Data Centre via www.ccdc.cam.ac.uk/data_request/cif.

Acknowledgements

J.R. thanks CONACyT de México (registro 113226) for a pre-doctoral fellowship. We acknowledge AMNA European project for financial support. We acknowledge the European Synchrotron Radiation Facility for provision of synchrotron radiation facilities and we thank Dr. Gavin Vaughan for recording the data and solving the structure of ligand **1b** (ESRF experiment CH-2474, beamline ID11). We thank Dr. Raymonde Baltenweck-Guyot for mass spectrometric analyses.

References and notes

- (a) Lehn, J.-M. *Chem.—Eur. J.* **2000**, *6*, 2097–2102; (b) Lehn, J.-M. *Proc. Natl. Acad. Sci. U.S.A.* **2002**, *99*, 4763–4768.
- See, for example: (a) Baxter, P. N. W.; Khoury, R. G.; Lehn, J.-M.; Baum, G.; Fenske, D. *Chem.—Eur. J.* **2000**, *6*, 4140–4148; (b) Baum, G.; Constable, E. C.; Fenske, D.; Housecroft, C. E.; Kulke, T. *Chem. Commun.* **1998**, 2659–2660; (c) Mamula, O.; Lama, M.; Stoeckli-Evans, H.; Shova, S. *Angew. Chem., Int. Ed.* **2006**, *45*, 4940–4944; (d) Funeriu, D. P.; Lehn, J.-M.; Fromm, K. M.; Fenske, D. *Chem.—Eur. J.* **2000**, *6*, 2103–21011; (e) Funeriu, D. P.; Rissanen, K.; Lehn, J.-M. *Proc. Natl. Acad. Sci. U.S.A.* **2001**, 10546–10551.
- (a) Barboiu, M.; Lehn, J.-M. *Proc. Natl. Acad. Sci. U.S.A.* **2002**, *99*, 5201–5206; (b) Stadler, A.-M.; Kyritsakas, N.; Lehn, J.-M. *Chem. Commun.* **2004**, 2024–2025.
- Ramírez, J.; Stadler, A.-M.; Kyritsakas, N.; Lehn, J.-M. *Chem. Commun.* **2007**, 237–239.
- Gardinier, K. M.; Khoury, R. G.; Lehn, J.-M. *Chem.—Eur. J.* **2000**, *6*, 4124–4131.
- Schmitt, J.-L. Ph.D. Thesis, Université Louis Pasteur, Strasbourg, 2004.
- Stadler, A.-M. Ph.D. Thesis, Université Louis Pasteur, Strasbourg, 2004. For helical wrapping of quinquepyridine and bishydrazones around metal ions see, for example: (a) Wester, D.; Palenik, G. J. *J. Chem. Soc., Chem. Commun.* **1975**, 74–75; (b) Constable, E. C.; Drew, M. G. B.; Forsyth, G.; Ward, M. D. *J. Chem. Soc., Chem. Commun.* **1988**, 1450–1451; (c) Buenzli, J.-C. G.; Piguet, C. *Chem. Rev.* **2002**, *102*, 1897–1928; (d) Constable, E. C. *Prog. Inorg. Chem.* **1994**, *42*, 67–137; (e) Albrecht, M. *Chem. Rev.* **2001**, *101*, 3457–3497.
- (a) For a review on grid-like complexes, see: Ruben, M.; Rojo, J.; Romero-Salguero, F. J.; Uppadine, L. H.; Lehn, J.-M. *Angew. Chem.* **2004**, *116*, 3728–3747; *Angew. Chem., Int. Ed.* **2004**, *43*, 3644–3662; See also: (b) Rojo, J.; Romero-Salguero, F. J.; Lehn, J.-M.; Baum, G.; Fenske, D. *Eur. J. Inorg. Chem.* **1999**, 1421–1428; (c) Ramírez, J.; Stadler, A.-M.; Harrowfield, J.; Brelot, L.; Rissanen, K.; Lehn, J.-M. *Z. Anorg. Allg. Chem.* **2007**, *633*, 2435–2444.
- Stadler, A.-M.; Kyritsakas, N.; Graff, R.; Lehn, J.-M. *Chem.—Eur. J.* **2006**, *12*, 4503–4522.
- Barboiu, M.; Lehn, J.-M. *Rev. Chim. (Bucarest)* **2006**, *57*, 909–914.
- For metal ion binding by the tren ligand, see: Zipp, S. G.; Zipp, A. P.; Madan, S. K. *Coord. Chem. Rev.* **1974**, *14*, 29–45; For similar use of the tren ligand, see: Stadler, A.-M.; Kyritsakas, N.; Vaughan, G.; Lehn, J.-M. *Chem.—Eur. J.* **2007**, *13*, 59–68.
- (a) Menicagli, R.; Samaritani, S.; Zucchini, V. *Tetrahedron* **2000**, *56*, 9705–9711; (b) Pitts, W. J.; Guo, J.; Murali Dhar, T. G.; Shen, Z.; Gu, H. H.; Watterson, S. H.; Bednarz, M. S.; Chen, B.-C.; Barrish, J. C.; Bassolino, D.; Cheney, D.; Fleener, C. A.; Rouleau, K. A.; Hollenbaugh, D. L.; Iwanowicz, E. J. *Bioorg. Med. Chem. Lett.* **2002**, *12*, 2137–2140.
- Harris, R. L. N. *Synthesis* **1981**, 907–908.
- García, A. M.; Bassani, D. M.; Lehn, J.-M.; Baum, G.; Fenske, D. *Chem.—Eur. J.* **1999**, *5*, 1234–1238.